

Liquid wall flow in counter-current column apparatuses for absorption processes with random packings

Chr. B. Boyadjiev¹, D. B. Dzhonova^{1*}, P. G. Popova-Krumova¹, K. V. Stefanova¹, A. N. Pavlenko², V. E. Zhukov², E. Yu. Slesareva²

¹*Institute of Chemical Engineering at the Bulgarian Academy of Sciences, Acad. G. Bonchev Str. Bl.103, Sofia 1113, Bulgaria,*

²*Kutateladze Institute of Thermophysics, Siberian Branch of the Russian Academy of Sciences, Lavrentyeva, 1, 630090, Novosibirsk, Russia*

Received: August 12, 2020; Accepted: August 21, 2020

Absorption processes are widely applied in chemical engineering. Important modern applications are fuel production and purification of waste gases and liquids for environment protection and production of valuable substances. Packed columns are typical apparatuses for these processes. Their efficient operation is strongly dependent on the regular distribution of the liquid and gas phase. The formation of a liquid wall flow is one of the main reasons for large-scale maldistribution in packed beds. The prediction of the liquid maldistribution is needed for evaluation of mass transfer efficiency. The present work uses a new approach to model the liquid wall flow in different types of random packings. The model results, in agreement with experimental data, show the effect of important operation parameters on the wall flow development along the column. A maldistribution parameter is calculated as a base for comparison of liquid maldistribution in packings. The present method for evaluation of the wall flow is intended for further modeling of separation efficiency in packed columns.

Keywords: Packed columns, absorption, random packings, liquid maldistribution, wall flow, mass transfer efficiency.

INTRODUCTION

When designing an absorption column, the packed bed should ensure the desired absorption rate at the lowest capital and operating cost, high mass transfer efficiency and low pressure drop. The selection of packings for a desired separation process passes through calculation of the most economic geometry with smallest dimensions, which will supply the highest mass transfer conditions. Many types of packings are designed in order to achieve the desired high mass transfer efficiency of the packed bed. Random packings are classified in 4 generations [1], the modern one being represented by web-like packings with open structure. They possess high-performance characteristics which provide for good hydrodynamic conditions and intensive mass transfer. The packing height can be calculated based on Height of a Transfer Unit (HTU) and Number of Transfer Units (NTU) [2], HTU being a measure of the mass transfer efficiency of the packing for the specific separation, based on the mass transfer rate between the liquid and vapor phase. The efficiency can also be evaluated by the concept of Height Equivalent to a Theoretical Plate (HETP), which treats a packed column as a series of equivalent equilibrium stages.

The maldistribution of the phases in a packed column has a deteriorating effect on the mass

transfer efficiency. It is specified as small-scale and large-scale maldistribution. It has been shown [3] that in random and structured packings the small-scale maldistribution, in the scale of a packing element, is characterized by the deviation of the local flow rates in the main body of the packed bed. The small-scale maldistribution results from the packing geometry and structure and it cannot be eliminated. Its harmful effect on separation efficiency is expected to be partially compensated by radial mixing between phases. This maldistribution intensifies with the packing depth until reaching a stable pattern of “natural flow” [3]. The large-scale maldistribution develops along the column wall as a result of insufficient irrigation or by development of a wall flow. It cannot be easily compensated by radial mixing. The initial distribution can be improved by proper design of the liquid distributor. The wall flow can be minimized by special elements, like deflecting rings [4] or by liquid redistribution devices [5] at a certain distance along the column. Hoek *et al.* [3] showed that structured packings are characterized by much more regular liquid flow patterns and the flow equilibrium between the bulk of the column and the wall zone is established at lower depth.

The separation system can be less or more sensitive to maldistribution [6], which means that with one and the same maldistribution the effect on efficiency differs from system to system and in the even different sections of the column. It is pointed

* To whom all correspondence should be sent:

E-mail: dzhonova@bas.bg

in [3], that maldistribution becomes relatively more detrimental for larger NTU, which has led to the industrial practice to redistribute the liquid at column height equivalent with 10-20 theoretical stages [5].

There are numerous techniques to evaluate the effect of maldistribution on the mass transfer process available in literature. The methods of parallel columns assume that liquid maldistribution results in divergences of the liquid-to-gas flow ratios and the packing can be subdivided into several (3-100) parallel bed sections (3 columns in [5] and [7]). Some “by-pass” methods are reviewed in [6]. They assume that part of the phase does not participate in the mass transfer [8], which damages the final product. There are models which obtain the flow pattern and the concentrations in each point of the packed bed, generally using CFD techniques [9, 10]. Yin [9] predicted HETP at good agreement with the experiment. His simulation tracked the effect of the loading of the phases on HETP. A widely applied approach to predict the flow pattern in the packed bed uses diffusion models [3, 11-13].

It is accepted that the large-scale maldistribution of the liquid phase is one of the main reasons for reduction in efficiency of absorption processes. The degree of maldistribution is independent of the gas flow in operation below the loading point. In order to obtain data to predict the large-scale liquid maldistribution and control the wall flow, extensive studies have been carried out. For first generation packings, ceramic Raschig rings, Farid & Gunn [14] introduced and estimated experimentally the relative permeability of the wall and bulk regions of the column. They explained the liquid maldistribution with the effect of reduced porosity in a region of one packing element diameter from the wall.

Hoek *et al.* [3] presented the following stages of development of wall flow profiles along the bed depth: 1) Non liquid-covered wall zone; 2) Migration of liquid into non liquid-covered wall zone, based on radial spreading coefficient D_r ; 3) Flow of liquid from packing to the wall, proportional to the liquid flow in the packing near the wall; 4) Flow-back of liquid from the wall into the packing, proportional to the flow rate along the wall. The growth of the wall flow reaches equilibrium at a certain packing depth. They studied the distribution of water at absence of gas flow and different heights of several random (1st and 2nd generation) and structured packings of different materials.

Yin *et al.* [15] contributed to better understanding of liquid spreading in packed columns by investigating various factors affecting wall flow formation in stainless steel Pall rings [25]. They reported that at initial maldistribution, a higher packing layer was necessary for the development of a stable “natural flow” of the packing. With the increase of liquid flow rate, the liquid relative wall flow was reduced slightly and the bed height required for the liquid to reach its equilibrium state was also reduced. In preloading regimes, the effect of gas flow rate on liquid distribution was insignificant. The liquid surface tension was found to have little or no effect on liquid distribution. The higher liquid viscosity reduces both the liquid radial spreading and the wall flow.

The aim of the present work is to demonstrate with different random packings a new approach developed theoretically in [16] for evaluation of the amount of liquid in the wall flow. The model equation suggested there is used to predict the wall flow thickness in random packings for further assessment of the effect of liquid maldistribution on mass transfer efficiency. It is used to reveal the factors affecting the relative wall flow rate and the wall flow thickness.

METHODS

The volume of the liquid flowing on the column wall participates in the absorption process only with its outer surface. The amount of liquid entering the wall flow by-passes the core volume of intensive mixing between the phases and leads to a reduction in the mass transfer rate of the liquid phase.

As suggested in [16], the thickness of the wall layer of liquid in columns with random packings can be represented by an asymptotic function $\delta(z)$:

$$\delta(z) = \frac{z}{a+bz}, \quad \delta(0) = 0, \quad \delta(\infty) = \frac{1}{b} = \delta_{\max}, \quad (1)$$

where z is the axial coordinate and the parameters (a , b) are determined from experimental data of the flow rate of the liquid flowing along the wall of the column.

The amount of liquid by-passing the absorption process can be represented by the wall flow volume V [m^3m^{-1}] per unit circumference of the column, which is determined by integrating (1):

$$V = \int_0^l \frac{z}{a+bz} dz = \frac{a}{b^2} \left(\frac{b}{a} l - \ln \frac{a+bl}{a} \right). \quad (3)$$

Width of the wall flow

In order to find the width of the wall flow $\delta(z)$, it is assumed that the average velocities of the liquid in the wall flow and in the bulk are:

$$\left(\frac{v_0}{2}, \frac{v_z^0 + v_0}{2} \right), \quad (4)$$

where v_0 [ms⁻¹] is the surface velocity of the wall liquid layer, $v_z^0 = \frac{Q_L}{\varepsilon_2 \pi r_0^2}$ [ms⁻¹] is the mean liquid velocity in the cross-section area occupied by the liquid, ε_2 - liquid volume (area) fraction, and Q_L [m³s⁻¹] - total liquid flow rate.

The flow rate of the wall flow $Q(z)$ per unit circumference of the column ($2\pi r_0$) is expressed in [16] by the average velocities of the liquid on the wall and in the bulk as a subtraction of the bulk flow rate from the total liquid flow rate in the column, resulting in a quadratic equation. Its positive root is the following relation:

$$\delta(z) = \frac{1}{2} \left\{ -r_0' + \left(r_0'^2 + \frac{8r_0 Q(z)}{v_z^0} \right)^{1/2} \right\}, \quad (5)$$

where

$$r_0' = \frac{v_z^0 \varepsilon_2 r_0 + 2Q(z) \varepsilon_2 - 2Q(z)}{v_z^0 \varepsilon_2}. \quad (6)$$

The obtained experimental values of $\delta(z)$ by Eq. (5) allow to determine the parameters (a , b) in Eq. (1) by minimizing the function of the least square differences between model and experimental data.

Maldistribution parameter

The calculation of the thickness of the wall flow in random packings enables to determine the variable radius r of the core volume of the packed column, where the absorption process takes place:

$$r = r_0 - \delta(z). \quad (7)$$

After obtaining (a , b) and $\delta(z)$ by Eq. (1), it is possible to calculate the equilibrium length of the

liquid layer on the wall l_e , when the layer thickness reaches 95% of its maximal value $\delta_{\max} = b^{-1}$ [16].

$$l_e = \frac{19a}{b} \quad (8)$$

The equilibrium volume of the wall flow V_e at $l=l_e$ is obtained directly from Eq. (3):

$$V_e = 16 \frac{a}{b^2}. \quad (9)$$

A maldistribution parameter E , suggested in [16], is used for comparison of the wall flow formation in different packings, for evaluation of their potential for separation efficiency:

$$E = V_e^{-1}. \quad (10)$$

RESULTS AND DISCUSSION

The aforementioned calculation procedure [16] is applied to various types and sizes of random packings of different material at countercurrent gas and liquid flows of different loads, including in absence of gas flow. The experimental conditions are presented in Table 1. All experiments are carried out at a semi-industrial scale of the equipment, system air-water, uniform initial distribution of the phases, and regimes under the loading point. The constants (a , b) in the function of the wall flow thickness, with the respective coefficients of determination R^2 of the regression, and the maldistribution parameter are presented in Table 2. For the purpose of comparison, the wall flow volume and the maldistribution parameter are calculated per one-meter height of the packed bed:

$$V_e^* = V_e \cdot l_e^{-1}, \\ E^* = V_e^*^{-1}$$

Table 1. Operational conditions and parameters of considered cases

N	Packing [source]	Column radius r_0 [m]	Liquid load L_0 [m ³ m ⁻² s ⁻¹]	Gas load G_0 [m ³ m ⁻² s ⁻¹]	Maximal bed height [m]	Liquid volume fraction ε_2 [source]
1	Metal Raschig-Super-Ring 1.5, (RSRM) Dzhonova <i>et al.</i> [17]	0.235	12e-03	0	1.4	0.009 [18]
2	Metal Pall ring 25, Yin <i>et al.</i> [15]	0.3	2.9e-03	0.625	3	0.034 [19]
3	Metal Pall ring 25, Yin <i>et al.</i> [15]	0.3	6.66e-03	0.625	3	0.062 [19]
4	Plastic Pall ring 50 Kouri and Sohlo [11]	0.25	2.5e-03	0	3.5	0.022 [19]
5	Plastic Pall ring 50 Kouri and Sohlo [11]	0.25	2.5e-03	1.67	3.5	0.022 [19]
6	Plastic Pall ring 50 Kouri and Sohlo [11]	0.25	10e-03	0	3.5	0.053 [19]
7	Plastic Pall rings 50 Kouri and Sohlo [11]	0.25	10e-03	1.67	3.5	0.053 [19]

Table 2. Model constants for the wall flow thickness and maldistribution parameter

N	Q_L [m ³ s ⁻¹]	a	b [m ⁻¹]	R^2	δ_{\max} [m]	l_e [m]	V_e [m ³ m ⁻¹]	V_e^* [m ³ m ⁻²]	E^* [m ⁻³ m ²]
1	0.00208	2330.80	561.23	0.99	0.0018	78.91	0.1184	0.0015	666.46
2	0.00082	415.63	384.10	0.93	0.0026	20.56	0.0451	0.0022	456.12
3	0.00188	205.78	259.08	0.89	0.0039	15.09	0.0491	0.0033	307.65
4	0.00049	222.62	318.65	0.80	0.0031	13.27	0.0351	0.0026	378.39
5	0.00049	147.39	309.05	0.84	0.0032	9.06	0.0247	0.0027	367.00
6	0.00196	40.49	251.16	0.59	0.0040	3.06	0.0103	0.0034	298.26
7	0.00196	27.79	175.23	0.73	0.0057	3.01	0.0145	0.0048	208.08

Packing 1

RSRM is a modern 4th generation packing of open structure. In [17] the data on liquid distribution in RSRM 1.5 are obtained at one phase flow of water by the liquid collecting method with 7 concentric annular collecting sections, at the bottom of the packed bed. The wall flow section was 5 mm wide, with an area of 4.21% of the total cross-section area. The relative wall flow rate was measured at three liquid loads, (5e-03 m³m⁻²s⁻¹, 8e-03 m³m⁻²s⁻¹ and 12e-03 m³m⁻²s⁻¹), at different packing heights 0.3-1.4 m. The initial distribution was uniform and the peripheral drip points were at a distance from the wall to prevent formation of a wall flow immediately after the distributor. The set-up and measuring procedure are reported in detail in [17, 20]. It was found that in the studied regimes, the effect of the liquid load on the liquid distribution can be accepted negligible [20]. The model function was determined for a liquid load of 12e-03 m³m⁻²s⁻¹. The model data are in good agreement with the experiment, as can be seen in Fig. 1.

Packing 2

Metal Pall ring is a widely used well studied random packing of second generation. Yin *et al.* [15] studied a 25.4 mm stainless steel Pall ring at different water and air flow rates. They measured the liquid distribution by the liquid collecting method at different packed bed heights. The wall collecting zone was 3.12% of total column (4.7 mm wide) cross-sectional area. The set-up and measuring procedure are reported in [15]. The model data are compared to the experiment in Fig. 2. Fig. 2 demonstrates that with the increase of liquid flow rate, the liquid relative wall flow and the packing bed depth for equilibrium state are reduced, while the wall liquid layer thickness is increased.

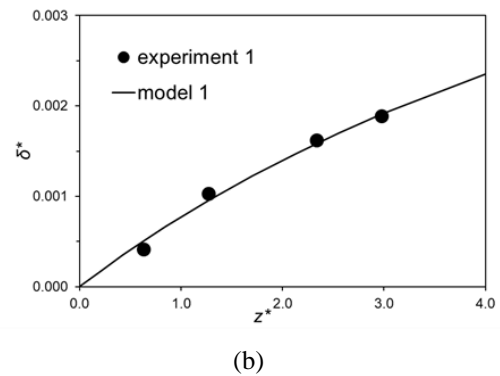
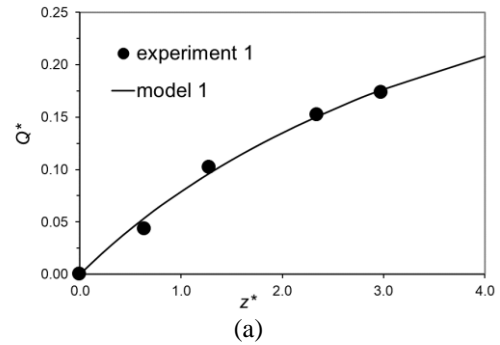


Fig.1. Wall flow in RSRM1.5, $L_0=12e-03$ m³m⁻²s⁻¹: a) Relative wall flow rate, b) Relative layer thickness

Packing 3

Plastic pall ring 50 was studied by Kouri and Sohlo [11]. The authors reported data for the liquid and gas flow patterns and the liquid wall flow in random packings, measured by the liquid collecting method with annular wall collecting section 15 mm wide with an area of 11.64% of the column cross-section. The comparison of the model to the experimental data in Fig. 3 shows good agreement. Fig. 3 demonstrates the effect of the gas phase. The presence of a countercurrent gas flow leads to an increase in the relative wall flow, the equilibrium depth, and the wall layer thickness, which implies to a local overloading. With the increase of the liquid load, the relative wall flow and its equilibrium depth is reduced, while the layer thickness is increased (in conformity with the dependencies shown in Fig. 2).

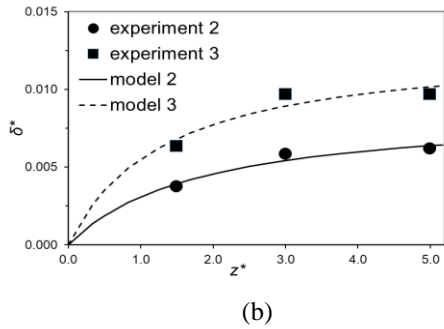
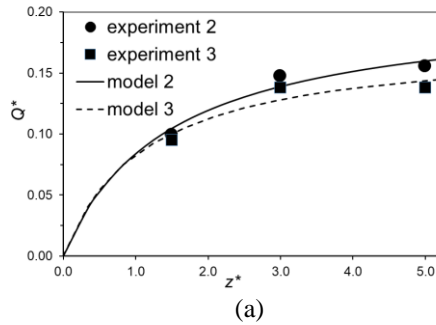


Fig. 2. Wall flow in a metal Pall ring 25, 2- $L_0=2.9 \times 10^{-3} \text{ m}^3 \text{ m}^{-2} \text{ s}^{-1}$, $G_0=0.625 \text{ m}^3 \text{ m}^{-2} \text{ s}^{-1}$, 3- $L_0=6.66 \times 10^{-3} \text{ m}^3 \text{ m}^{-2} \text{ s}^{-1}$, $G_0=0.625 \text{ m}^3 \text{ m}^{-2} \text{ s}^{-1}$: a) Relative wall flow rate, b) Relative layer thickness.

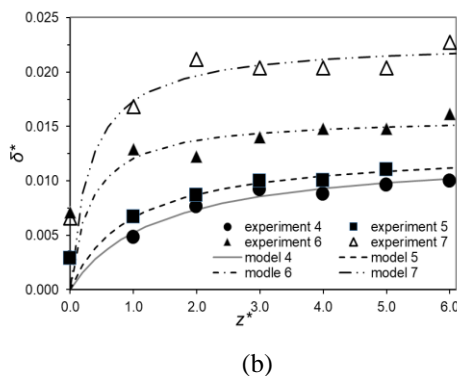
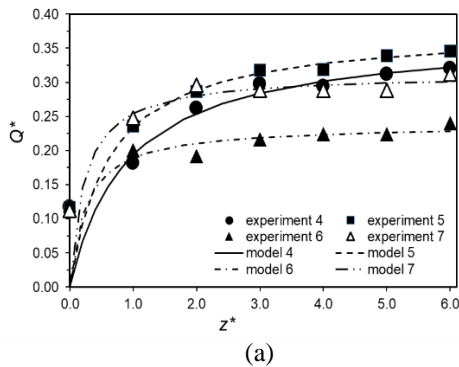


Fig. 3. Wall flow in a plastic Pall ring 50: 4- $L_0=2.5 \times 10^{-3} \text{ m}^3 \text{ m}^{-2} \text{ s}^{-1}$, $G_0=0 \text{ m}^3 \text{ m}^{-2} \text{ s}^{-1}$, 5- $L_0=2.5 \times 10^{-3} \text{ m}^3 \text{ m}^{-2} \text{ s}^{-1}$, $G_0=1.67 \text{ m}^3 \text{ m}^{-2} \text{ s}^{-1}$, 6- $L_0=10 \times 10^{-3} \text{ m}^3 \text{ m}^{-2} \text{ s}^{-1}$, $G_0=0 \text{ m}^3 \text{ m}^{-2} \text{ s}^{-1}$; 7- $L_0=10 \times 10^{-3} \text{ m}^3 \text{ m}^{-2} \text{ s}^{-1}$, $G_0=1.67 \text{ m}^3 \text{ m}^{-2} \text{ s}^{-1}$: a) Relative wall flow rate, b) Relative layer thickness

Comparing the maldistribution parameter E^* (Table 2), it can be seen that it is highest for RSRM,

which speaks for a smaller wall flow and small degree of liquid maldistribution in this packing. This is in agreement with the data in [5], where a maldistribution factor was used to show a lower degree of liquid maldistribution for RSRM packing in comparison to other packings of older generations.

CONCLUSIONS

A new model of wall flow in random packings was applied for evaluation of the liquid maldistribution. A maldistribution parameter was calculated for comparison of packings of different type, size and material for potential to develop wall flow, which is unfavorable for separation efficiency. The model was used to show the effect of liquid and gas load on wall flow build-up along the column.

The high-performance metal packing RSRM has the highest maldistribution parameter per unit height of the packed bed. It has the smallest relative wall flow and equilibrium thickness of the liquid layer on the wall, and the greatest packing depth for reaching equilibrium state.

The plastic Pall ring 50 displays the biggest relative wall flow and equilibrium layer thickness which is reached at the smallest packing depth.

The increase of the liquid load leads to a reduction in the relative wall flow and equilibrium packing depth, but to an increase in the liquid layer thickness and its equilibrium value.

In presence of a gas flow, the relative liquid wall flow and equilibrium layer thickness are increased, while the equilibrium packing depth is reduced.

The presented approach for evaluation of liquid maldistribution in random packings can be used in future development of a model for prediction of the flow pattern and separation efficiency.

Acknowledgements: This work was partially supported by the National Science Fund of Bulgaria, contract KP 06 RUSIA-3/27.09.2019, the Russian Foundation for Basic Research contract # 19-58-18004, and the Bulgarian Ministry of Education and Science under the National Research Programme “Low-carbon energy for transport and domestic use (EPLUS)” (approved by DCM No. 577/17.08.2018 and Grant Agreement DOI-214/28.11.2018).

NOMENCLATURE

a, b - constants in the model function (1);
 D_r - radial liquid spreading coefficient, m;
 $E = V^l$ - maldistribution parameter, $m \cdot m^{-3}$;
 $E^* = V^{*l}$ - maldistribution parameter per one-meter height of the packed bed, $m^2 m^{-3}$;
 G_0 - gas load, $m^3 m^{-2} s^{-1}$;
 L - packing height, m;
 L_0 - liquid load, $m^3 m^{-2} s^{-1}$;
 Q_L - total liquid flow rate, $m^3 s^{-1}$;
 $Q(z)$ - flow rate of the wall flow per unit circumference of the column, $m^3 m^{-1} s^{-1}$;
 $r = r_0 - \delta(z)$ - variable radius of the core volume of the packed column where the absorption process takes place, m;
 r_0 - column radius, m;
 R^2 - coefficients of determination;
 v_0 - surface velocity of the wall liquid layer, ms^{-1} ;
 v_z^0 - mean liquid velocity in the cross-section area occupied by the liquid, ms^{-1} ;
 V - wall flow volume per unit circumference of the column, $m^3 m^{-1}$;
 $V_e^* = V_e \cdot l_e^{-1}$ - wall flow volume per unit circumference per one-meter height of the packed bed, $m^3 m^{-2}$;
 z - axial coordinate, m;
 $z^* = z(2r_0)^{-1}$ - dimensionless axial coordinate;
Greek letters:
 δ - thickness of the liquid layer on the column wall, m;
 $\delta^* = \delta r_0^{-1}$ - relative thickness of the liquid layer on the wall;
 δ_{max} - maximal thickness of the liquid layer on the wall at equilibrium state, m;
 ε_2 - liquid volume (area) fraction;
Subscripts:
 0 - at inlet;
 e - at equilibrium state;
Abbreviations:
 CFD - Computational Fluid Dynamics;
 HETP - Height Equivalent to a Theoretical Plate;
 HTU - Height of a Transfer Unit;
 NTU - Number of Transfer Units;
 RSSRM - metal Raschig-Super-Ring packing.

REFERENCES

1. M. Schultes, *Trans IChemE*, **81**, Part A, 48 (2003).
2. R. Billet, M. Schultes, *Trans. IChemE*, **77**, Part A, 498 (1999).
3. P. J. Hoek, J. A. Wesselingh, F. J. Zuiderweg, *Chem. Eng. Res. Des.*, **64**(6), 431(1986).
4. N. Kolev, R. Darakchiev, Bulg. Patent No. 18018 (1972).
5. M. Schultes, *Ind. Eng. Chem. Res.*, **39**, 1381 (2000).
6. J. F. Billingham, M. J. Lockett, *Trans. IChemE*, **80**, Part A, 373 (2002).
7. M. J. Lockett, J. F. Billingham, *Trans. IChemE*, **81**, Part A, 131 (2003).
8. B. Hanley, *Separ. Purif. Technol.*, **16**, 7 (1999).
9. F. Yin, Liquid maldistribution and mass transfer efficiency in randomly packed distillation columns, PhD Thesis, Univ. Alberta, 1999.
10. Yang, CFD modeling of multiphase countercurrent flow in packed bed reactor for carbon capture, PhD Thesis, Univ. Kentucky, 2015.
11. R. Kouri, J. Sohlo, *Chem. Eng. J.*, **61**, 95 (1996).
12. V. Stanek, V. Kolar, *Collect. Czech. Chem. Commun.*, **38**, 2865 (1973).
13. T. St. Petrova, Kr. A. Semkov, D. B. Dzhonova, *Chem Eng. Trans.*, **70**, 1051 (2018).
14. M. M. Farid, D. J. Gunn, *Chem. Eng. Sci.*, **33**(9), 1221 (1978).
15. F. Yin, Z. Wang, A. Afacan, K. Nandakumar, K. T. Chuan, *Can. J. Chem. Eng.*, **78**(3), 449 (2000).
16. Chr. B. Boyadjiev, D. B. Dzhonova, K. V. Stefanova, St. P. Panyovska, P. G. Popova, A. N. Pavlenko, V. E. Zhukov, E. Yu. Slesareva, *J. of Phys. Conf. Ser.*, in press (2020).
17. D. Dzhonova-Atanasova, T. Petrova, S. Darakchiev, P. Panayotova, Sv. Nakov, R. Popov, Kr. Semkov, *Sci. Works of Univ. Food Tech.* **LXI**, 644 (2014).
18. Sv. Ts. Nakov, D. B. Dzhonova, E. N. Razkazova, *Bulg. Chem. Commun.*, **52**, Spec. Issue, in press (2020).
19. J. Mackowiak, *Fluid Dynamics of Packed Columns*, Springer, Heidelberg, 2010, p. 192.
20. D. B. Dzhonova-Atanasova, T. St. Petrova, Kr. A. Semkov, S. R. Darakchiev, K. V. Stefanova, Sv. Ts. Nakov, R. G. Popov, *Chem. Eng. Trans.*, **70**, 2077 (2018).